Available online at www.sciencedirect.com
ScienceDirect
Trans. Nonferrous Met. Soc. China 24(2014) 2920−2929
Transactions of Nonferrous Metals Society of China
www.tnmsc.cn

# Mechanical properties and electronic structures of $MgCu_2$, $Mg_2Ca$ and $MgZn_2$ Laves phases by first principles calculations

Ping-li MAO, Bo YU, Zheng LIU, Feng WANG, Yang JU

School of Materials Science and Engineering, Shenyang University of Technology, Shenyang 110870, China

Received 8 October 2013; accepted 14 January 2014

**Abstract:** Mechanical properties and electronic structure of $MgCu_2$, $Mg_2Ca$ and $MgZn_2$ phases were investigated by means of first principles calculations from CASTEP program based on density functional theory (DFT). The calculated lattice parameters are in good agreement with the experimental and literature values. The calculated heat of formation and cohesive energies showed that $MgCu_2$ has the strongest alloying ability and structural stability. Elastic constants of $MgCu_2$, $Mg_2Ca$ and $MgZn_2$ were calculated, and the bulk moduli, shear moduli, elastic moduli and Poisson ratio were derived. The calculated results show that $MgCu_2$, $Mg_2Ca$ and $MgZn_2$ are all ductile phases. Among the three phases, $MgCu_2$ has the strongest stiffness and the plasticity of $MgZn_2$ phase is the best. Melting points of the three phases were predicted using cohesive energy and elastic constants. Density of states (DOS), Mulliken population, electron occupation number and charge density difference were discussed. Finally, Debye temperature was calculated and discussed.

**Key words:** magnesium alloy; $MgCu_2$; $Mg_2Ca$; $MgZn_2$; Laves phases; electronic structure; mechanical property; Debye temperature

## 1 Introduction

Magnesium alloys have many advantages, such as low density, high specific strength and stiffness, good damping capacity and machinability, easy recycling, and have been widely used in aerospace industry, automotive industry, 3C products, national defense and other fields. Magnesium is the lightest metal structural material, known as the "green" engineering material [1,2]. However, due to the low heat resistance, low strength and ductility, magnesium alloys are limited to the extensive use on the heat resistant structure parts. Zinc element is a commonly used alloying element in magnesium alloy, it has the same electrovalence and crystal structure with Mg and can form a large concentration solid solution with Mg [3].

In recent years, high-performance wrought magnesium alloys, especially Mg−Zn based alloys, have been received increasing attention. Mg−Zn binary alloys contain MgZn, $Mg_2Zn_3$, $MgZn_2$ and $Mg_2Zn_{11}$ phases, of which the most important strengthening phase is $MgZn_2$ [4,5]. The study shows that grain refinement can significantly improve the strength and ductility of magnesium and its alloys [6]. In the Mg−Zn binary alloy, the grains can be significantly refined by adding light and inexpensive elements Ca, and also Ca element can increase the density of aging precipitates $MgZn_2$ phases, thereby improving the mechanical properties of the alloy [7]. Due to a potential performance of high temperature alloy, Mg−Zn−Ca alloys have been gained widespread attention [8,9]. Alloying is an effective method to improve the microstructure and mechanical properties of magnesium alloys. LUO and PEKGUCERYUZ [10] showed that by adding Cu, the strength and plasticity of magnesium alloys can be improved by forming $MgCu_2$ phase. QIU et al [11] studied the amorphous forming ability and mechanical properties in Mg−Zn−Ca alloy by adding Cu based on the experimental method. SENKOV and SCOTT [12] studied the formation and thermal stability of Ca−Mg−Zn and Ca−Mg−Zn−Cu bulk metallic glasses. LIU et al [13] investigated the structural and electronic properties of $MgCu_2$ Laves phase under pressure by first principles calculations. However, no systematic theoretical investigations have been reported on electronic structure, mechanical properties and Debye temperature of $MgCu_2$, $Mg_2Ca$ and $MgZn_2$ Laves phases in Cu alloyed Mg−Zn−Ca alloy by first principles

**Foundation item:** Project (2013201018) supported by Scientific and Technological Project of Liaoning Province, China
**Corresponding author:** Ping-li MAO; Tel: +86-24-25497131; E-mail: pinglimao@yahoo.com
DOI: 10.1016/S1003-6326(14)63427-0

calculations. The elastic constants of compounds have been used to determine the mechanical properties of the compounds, and due to the experimental inconvenience, and the elastic constants of metals have been investigated by quantum mechanics method based on density functional theory, giving some satisfactory results for the calculated bulk modulus, shear modulus and other elastic constants in recent years [14]. Therefore, using the theory method to study elastic constants ($C_{ij}$) of $MgCu_2$, $Mg_2Ca$ and $MgZn_2$ is feasible.

In the present work, the first principles calculations are used to investigate the structural, elastic and electronic properties of the binary $MgCu_2$, $Mg_2Ca$ and $MgZn_2$ Laves phases. The melting points and Debye temperatures are also calculated. The obtained results are compared with the available experimental and theoretical values.

## 2 Computational method

Cambridge sequential total energy package (CASTEP), a first principles plane wave pseudo-potentials method based on density function theory (DFT) [15], is used for the calculations. Generalized gradient approximation (GGA) of Perdew–Burke–Ernzerhof (PBE) [16] is used to describe the exchange-correlation energy function. The ultrasoft pseudo-potential [17] is used to describe the interaction between ion core and valence electron. The outermost electron configuration for Mg is $3s^2$, and others are described by $4s^2$, $3d^{10}$ for Ca, $4s^2$ for Zn, $3d^{10}$, $4s^1$ for Cu, respectively. The parameters that affect the calculation accuracy are kinetic energy cutoff and the number of *k*–points network in brillouin zone; the cut-off energy of plane wave is set to 380 eV; the Monkhost–Pack scheme with a *k*–points separation for $Mg_2Ca$ and $MgZn_2$ are 6×6×4, for $MgCu_2$ is 6×6×6, respectively. Geometry optimization is carried out under the electron relaxation until the total energy convergence value is $5.0\times10^{-8}$ eV/atom; the maximum Hellmann–Feynaman force is within 0.01 eV/Å; the maximum displacement is within $5\times10^{-4}$ Å; and the maximum stress is within 0.02 GPa.

The elastic constants of $MgCu_2$, $Mg_2Ca$ and $MgZn_2$ are calculated by the stress–strain method. The maximum strain amplitude is set to 0.003. The total energy convergence value is $1.0\times10^{-6}$ eV/atom, the maximum force is within 0.002 eV/Å, and the maximum displacement is within $1.0\times10^{-4}$ Å.

## 3 Results and discussion

### 3.1 Crystal structure and lattice constant

The crystal structures of $MgCu_2$, $Mg_2Ca$ and $MgZn_2$ are shown in Fig. 1. The structure parameters and lattice constants are listed in Tables 1 and 2. The calculated lattice constants are in good agreement with the experimental and other theoretical values, and the error is only 2%. The fairly good agreement between the theoretical and experimental values shows that the present calculations are highly reliable.

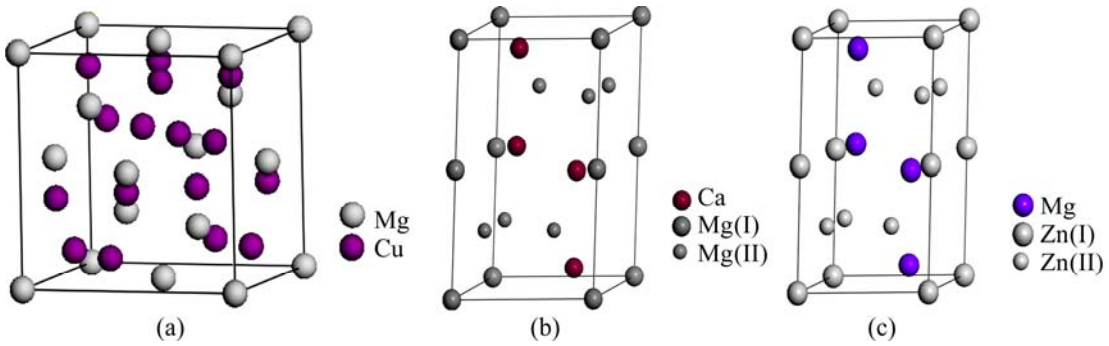


**Fig. 1** Crystal structures of $MgCu_2$ (a), $Mg_2Ca$ (b) and $MgZn_2$ (c)

**Table 1** Structure parameters of $MgCu_2$, $Mg_2Ca$ and $MgZn_2$

| Phase | Atom number in cell | Space group | Structure type | Pearson sign | Atom site |
|---|---|---|---|---|---|
| $MgCu_2$ | 24 | $Fd\bar{3}m$ (227) | C15 | cF24 | Cu: 16d (0.5, 0.5, 0.5); Mg: 8a (0.125, 0.125, 0.125) |
| $Mg_2Ca$ | 12 | *P*63/*mmc* (194) | C14 | hP12 | Ca: 4f (0.33, 0.67, 0.062); Mg: 2a (0, 0, 0); Mg: 6h (0.34, 0.17, 0.25) |
| $MgZn_2$ | 12 | *P*63/*mmc* (194) | C14 | hP12 | Mg: 4f (0.33, 0.67, 0.062); Zn: 2a (0, 0, 0); Zn: 6h (0.34, 0.17, 0.25) |

**Table 2** Equilibrium crystal parameters ($a$, $c$), unit cell volume ($V_0$) and density ($\rho$) of $MgCu_2$, $Mg_2Ca$ and $MgZn_2$

| Phase | Present | | | | Experimental | | Calculated | |
|---|---|---|---|---|---|---|---|---|
| | $a$/Å | $c$/Å | $V_0$/Å$^3$ | $\rho$/(g·cm$^{-3}$) | $a$/Å | $c$/Å | $a$/Å | $c$/Å |
| $MgCu_2$ | 7.06 | 7.06 | 351.789 | 5.72 | 7.04 [18] | 7.04 [18] | 7.07 [18], 7.01 [19] | 7.07 [18], 7.01 [19] |
| $Mg_2Ca$ | 6.24 | 10.14 | 342.209 | 1.72 | 6.22 [20] | 10.10 [20] | 6.23 [21] | 10.09 [21] |
| $MgZn_2$ | 5.23 | 8.47 | 199.922 | 5.15 | 5.21 [22] | 8.54 [22] | 5.16 [19] | 8.56 [19] |

### 3.2 Heat of formation and cohesive energies

Heat of formation of $MgCu_2$, $Mg_2Ca$ and $MgZn_2$ is calculated by formula as follows:

$$\Delta H = \frac{E_{\text{tot}}^{\text{AB}} - N_{\text{A}}E_{\text{solid}}^{\text{A}} - N_{\text{B}}E_{\text{solid}}^{\text{B}}}{N_{\text{A}} + N_{\text{B}}} \quad (1)$$

where $\Delta H$ is the heat of formation; $E_{\text{tot}}^{\text{AB}}$ is the total energy of $AB_2$ type intermetallic compounds; $E_{\text{solid}}^{\text{A}}$ and $E_{\text{solid}}^{\text{B}}$ are the energy per atom of pure elements A and B, respectively; $N_{\text{A}}$ and $N_{\text{B}}$ are the numbers of A and B atoms in unit cell, respectively. The calculated energies of Mg, Cu, Ca and Zn in solid states are −973.9652, −1476.5411, −1001.5392 and −1709.8504 eV/atom, respectively. Based on the results of $E_{\text{tot}}^{\text{AB}}$, $E_{\text{solid}}^{\text{A}}$ and $E_{\text{solid}}^{\text{B}}$, the calculated heat of formation of $MgCu_2$, $Mg_2Ca$ and $MgZn_2$ are listed in Table 3.

The structural stability of $MgCu_2$, $Mg_2Ca$ and $MgZn_2$ is investigated by means of cohesive energy. Generally, the cohesive energy is defined as the energy needed to decompose the compound into a single atom. Hence, the larger the calculated value is, the more stable the crystal structure is [25]. Cohesive energies ($E_{\text{coh}}$) of $MgCu_2$, $Mg_2Ca$ and $MgZn_2$ are calculated by expression as follows:

$$E_{\text{coh}} = \frac{E_{\text{tot}}^{\text{AB}} - N_{\text{A}}E_{\text{atom}}^{\text{A}} - N_{\text{B}}E_{\text{atom}}^{\text{B}}}{N_{\text{A}} + N_{\text{B}}} \quad (2)$$

where $E_{\text{atom}}^{\text{A}}$ and $E_{\text{atom}}^{\text{B}}$ are the energies of A and B atoms in the free state, respectively. The calculated energies of Mg, Cu, Ca and Zn in free states are −972.4847, −1472.8555, −999.6320 and −1708.6826 eV/atom, respectively. Based on the results of $E_{\text{tot}}^{\text{AB}}$, $E_{\text{atom}}^{\text{A}}$ and $E_{\text{atom}}^{\text{B}}$, the obtained results are also listed in Table 3.

As can be seen from Table 3, the calculated values in this work are in good agreement with the experimental and theoretical values, proving the reliability of the calculation methods. The negative heat values of formation of $MgCu_2$, $Mg_2Ca$ and $MgZn_2$ show that these phases can exist stably. The lower the heat of formation is, the stronger the forming ability is. From Table 3, it can be concluded that $MgCu_2$ phase has the strongest forming ability, then $MgZn_2$, finally $Mg_2Ca$.

From Table 3, we can know that $MgCu_2$ has the largest value of cohesive energy, and far larger than those of $Mg_2Ca$ and $MgZn_2$, indicating that $MgCu_2$ has the most stable structure, next $Mg_2Ca$, finally $MgZn_2$. Further analysis found that adding Cu into Mg–Zn–Ca alloy can improve the structural stability through forming $MgCu_2$ phase.

### 3.3 Mechanical properties

Elastic constants are often used to characterize the deformation resistant capacity to an externally applied stress. Cubic has three independent elastic constants as follows: $C_{11}$, $C_{12}$ and $C_{44}$, the corresponding stability criteria [26] are: $(C_{11}+2C_{12})/3>0$, $C_{11}-C_{12}>0$, $C_{44}>0$. The independent elastic constants for hexagonal are as follows: $C_{11}$, $C_{12}$, $C_{13}$, $C_{33}$ and $C_{44}$. The corresponding stability criteria [27] are: $C_{11}>0$, $C_{11}-C_{12}>0$, $C_{44}>0$, $>0, (C_{11}+C_{12})C_{33}-2C_{13}^2>0$.

The calculated elastic constants of $MgCu_2$, $Mg_2Ca$ and $MgZn_2$ are listed in Table 4. As can be seen from Table 4, the calculated results in this work are in good agreement with the experimental and theoretical values. Further analysis shows that the calculation results satisfy the stability criteria.

Bulk moduli ($B$) and shear moduli ($G$) of $MgCu_2$ are deduced by the following formula [30]:

$$B = \frac{1}{3}(C_{11} + 2C_{12}) \quad (3)$$

$$G = \frac{1}{5}(3C_{44} + C_{11} - C_{12}) \quad (4)$$

Bulk moduli ($B$) and shear moduli ($G$) of $Mg_2Ca$ and $MgZn_2$ are also estimated by Voigt–Reuss–Hill (VRH) approximation [30]. The Voigt bounds of $B$ and $G$ are

$$B_{\text{V}} = \frac{2}{9}\left(C_{11} + C_{12} + \frac{1}{2}C_{33} + 2C_{33}\right) \quad (5)$$

$$G_{\text{V}} = \frac{1}{30}(7C_{11} - 5C_{12} + 12C_{44} + 2C_{33} - 4C_{13}) \quad (6)$$

and the Reuss bounds are

$$B_{\text{R}} = \frac{(C_{11} + C_{12})C_{33} - 2C_{13}^2}{C_{11} + C_{12} + 2C_{33} - 4C_{13}} \quad (7)$$

$$G_{\text{R}} = \frac{5}{2}\frac{[(C_{11} + C_{12})C_{33} - 2C_{13}^2]C_{44}C_{66}}{3B_{\text{V}}C_{44}C_{66} + [(C_{11} + C_{12})C_{33} - 2C_{13}^2](C_{44} + C_{66})} \quad (8)$$

**Table 3** Heat of formation ($\Delta H$) and cohesive energy ($E_{coh}$) of $MgCu_2$, $Mg_2Ca$ and $MgZn_2$

| Phase | $\Delta H$/(kJ·mol$^{-1}$) | | | $E_{coh}$/(kJ·mol$^{-1}$) | | |
|---|---|---|---|---|---|---|
| | Present | Experimental | Calculated | Present | Experimental | Calculated |
| $MgCu_2$ | −13.28 | −11.70 [23] | −6.91 [23], −10.91 [24] | 297.83 | 284.70 [23] | 279.90 [23], 311.65 [19] |
| $Mg_2Ca$ | −11.34 | − | −12.44 [21] | 167.83 | − | 168.87 [21] |
| $MgZn_2$ | −11.47 | −10.90 [23] | −8.00 [23], −12.95 [19] | 134.22 | 142.50 [23] | 139.60 [23], 89.06 [19] |

**Table 4** Elastic constants ($C_{11}$, $C_{12}$, $C_{13}$, $C_{33}$ and $C_{44}$) of $MgCu_2$, $Mg_2Ca$ and $MgZn_2$

| Phase | Source | $C_{11}$/GPa | $C_{12}$/GPa | $C_{13}$/GPa | $C_{33}$/GPa | $C_{44}$/GPa |
|---|---|---|---|---|---|---|
| $MgCu_2$ | Present | 113.35 | 80.28 | − | − | 39.86 |
| | Cal. [19] | 129.06 | 83.16 | − | − | 43.73 |
| | Cal. [28] | 107.90 | 79.00 | − | − | 34.60 |
| $Mg_2Ca$ | Present | 51.43 | 22.31 | 14.73 | 58.51 | 14.32 |
| | Cal. [26] | 62.04 | 17.07 | 13.86 | 65.90 | 17.95 |
| $MgZn_2$ | Present | 91.25 | 87.27 | 28.62 | 147.59 | 20.21 |
| | Exp. [29] | 107.25 | 45.45 | 27.43 | 126.40 | 27.70 |
| | Cal. [19] | 91.25 | 85.27 | 23.38 | 198.31 | 24.88 |

Finally, the expressions of $B$ and $G$ are

$$B = \frac{1}{2}(B_V + B_R) \tag{9}$$

$$G = \frac{1}{2}(G_V + G_R) \tag{10}$$

where the subscripts V and R represent the Voigh and the Reuss, respectively. Further, elastic moduli ($E$), Poisson ratio ($v$) and anisotropic coefficient ($A$) are obtained according to the following formula [30]:

$$E = \frac{9BG}{3B + G} \tag{11}$$

$$\nu = \frac{3B - 2G}{2(3B + G)} \tag{12}$$

$$A = \frac{2C_{44}}{C_{11} - C_{12}} \tag{13}$$

The calculated results are listed in Table 5. The bulk moduli $B$, shear moduli $G$, elastic moduli $E$ and Poisson ratio $v$ of $MgCu_2$, $Mg_2Ca$ and $MgZn_2$ are shown in Fig. 2. From Table 5, it can be found that $E$ and $G$ are satisfied with the relation $G = E/2\ (1+v)$. The bulk moduli are usually assumed to be a measure of deformation resistant capacity upon applied pressure [31]. The larger the value of bulk modulus is, the stronger the capacity of the resist deformation is. From Fig. 2(a), we can conclude that the ability to resist deformation from strong to weak is $MgCu_2$, $MgZn_2$ and $Mg_2Ca$, respectively. Similarly, the shear modulus is a measure of resist reversible deformation by shear stress [31]. The larger the value is, the stronger the capacity of the resist shear deformation is. The calculated results demonstrate that $MgCu_2$ has the largest value, followed by $Mg_2Ca$ and $MgZn_2$. Hence, the deformation resistant capacity of $MgCu_2$ would be much stronger than that of $Mg_2Ca$ or $MgZn_2$. Besides, Poisson ratio is also a measure of the stability of the crystal against shear, which usually ranges from −1 to 0.5. The larger the Poisson ratio is, the better the plasticity is [27]. In Fig. 2(b), the calculated results demonstrate that $MgZn_2$ has the best plasticity because of the largest value of Poisson ratio, next $MgCu_2$, finally $Mg_2Ca$. Furthermore, elastic modulus is defined as the ratio between stress and strain, and it also provides a measure of stiffness of the solid materials. The larger the value is, the stiffer the material is. The calculated results show that the stiffness of $MgCu_2$ is the largest, then $Mg_2Ca$, and the last $MgZn_2$.

The ratio of shear moduli to bulk moduli ($G/B$) of polycrystalline phases is used to predict the brittle and ductile behavior of materials [31]. A high (low) $G/B$ value is associated with brittleness (ductility). The critical value, which is used to separate brittleness from ductility, is about 0.57. The $G/B$ values of $MgCu_2$, $Mg_2Ca$ and $MgZn_2$ are 0.33, 0.53 and 0.18, respectively. So, $MgCu_2$, $Mg_2Ca$ and $MgZn_2$ are all ductile. The $C_{12}-C_{44}$ value can also define the ductility (brittleness) of crystal [32,33]. If the value is positive, polycrystalline phases are ductile; otherwise, it is brittle. From Table 5, it can be obtained that $MgCu_2$, $Mg_2Ca$ and $MgZn_2$ are all ductile because the $C_{12}-C_{44}$ values are all positive, which is in good agreement with the previous ($G/B$) results. Hence, with the addition of Cu element, the plasticity of Mg−Zn−Ca alloy will be improved by forming the ductile phase of $MgCu_2$.

**Table 5** Bulk moduli ($B$), shear moduli ($G$), elastic moduli ($E$), elastic constants ($C_{ij}$), $G/B$, Poisson ratio ($v$) and anisotropic coefficient ($A$) of $MgCu_2$, $Mg_2Ca$ and $MgZn_2$

| Phase | Source | $B$/GPa | $G$/GPa | $E$/GPa | $G/B$ | $(C_{12}-C_{44})$/GPa | $v$ | $A$ |
|---|---|---|---|---|---|---|---|---|
| $MgCu_2$ | Present | 91.30 | 30.53 | 82.41 | 0.33 | 40.42 | 0.35 | 2.41 |
| | Cal. [19] | 98.46 | 35.42 | 63.89 | 0.36 | – | 0.39 | 1.91 |
| | Cal. [28] | 88.60 | 26.50 | 72.30 | 0.30 | – | – | – |
| $Mg_2Ca$ | Present | 29.43 | 15.72 | 40.04 | 0.53 | 7.99 | 0.27 | 0.98 |
| | Cal. [26] | 31.06 | 18.99 | 55.74 | 0.61 | – | 0.20 | 0.79 |
| $MgZn_2$ | Present | 68.79 | 12.65 | 35.77 | 0.18 | 67.06 | 0.41 | 10.15 |
| | Cal. [19] | 70.71 | 16.12 | 45.57 | 0.23 | – | 0.39 | 8.32 |

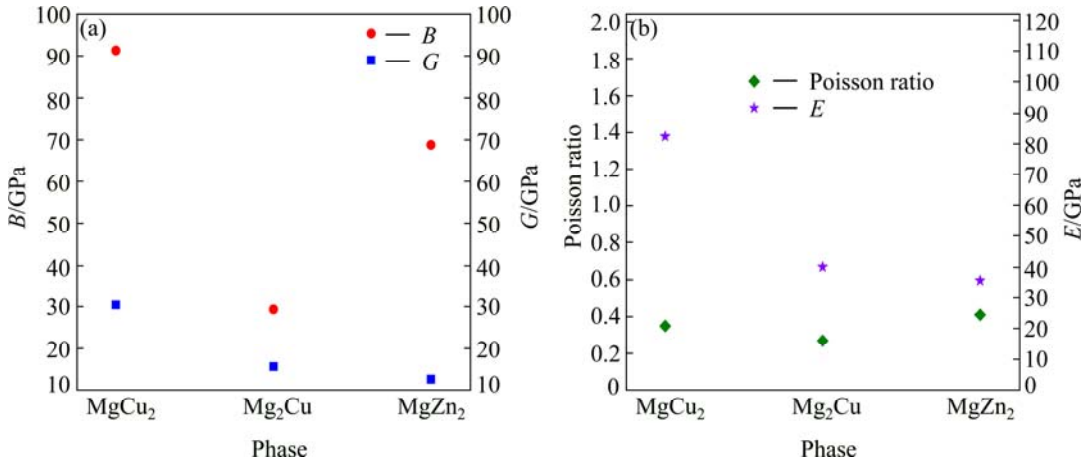


**Fig. 2** Bulk moduli ($B$), shear moduli ($G$) (a) and elastic moduli ($E$) and Poisson ratio ($v$) (b) of $MgCu_2$, $Mg_2Ca$ and $MgZn_2$

The melting point of the materials can be predicted using the cohesive energy and elastic constants based on empirical formula. LI et al [23] found that the melting point ($T_m$) and cohesive energy exbibit a linear relationship in binary intermetallic compounds as follows:

$$T_m=3.84867E_{coh} \quad (14)$$

For metal materials, the melting point and elastic constants shows a linear relationship as follows [19]:

$$T_m/K=553+5.91C_{11}\pm300 \quad (15)$$

$$T_m/K=354+4.50[1/3(2C_{11}+C_{33})]\pm300 \quad (16)$$

The melting point values of $MgCu_2$, $Mg_2Ca$ and $MgZn_2$ are shown in Fig. 3. It can be seen that the experimental values are in the predicting range of elastic constants (±300 K), but there is a certain deviation between the experimental value and the melting point predicted using the cohesive energy. We can know that the relative errors in melting points of $MgCu_2$, $Mg_2Ca$ and $MgZn_2$ by adopting cohesive energy are 4.87%, 34.76% and 40.14%, respectively. The relative errors calculated using elastic constants are 11.89%, 13.44% and 26.57% (by Eq. (15)), 20.94%, 39.79% and 1.61% (by Eq. (16)), respectively. Hence, for $MgCu_2$, $Mg_2Ca$ and $MgZn_2$, the melting point predicted using elastic constants is closer to the experimental values than using cohesive energy. There is a certain deviation between the predicted values and experimental values, but we can believe that the melting point of $MgCu_2$ is the highest among the three intermetallic compounds. The higher the melting point is, the better the structural stability at high temperature is. Hence, $MgCu_2$ has the best stability among the three intermetallic compounds.

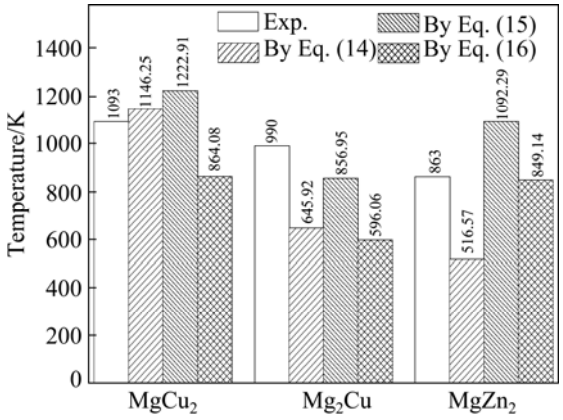


**Fig. 3** Melting temperatures of $MgCu_2$, $Mg_2Ca$ and $MgZn_2$

### 3.4 Electronic structures

The electronic structure is calculated to understand the bonding characteristics of $MgCu_2$, $Mg_2Ca$ and $MgZn_2$, and further reveal the mechanism about structural

stability and elastic properties. Structural stability of intermetallic compound is associated with its bonding electron orbits. For covalent bond, it depends on the depth and width of band gap near Fermi level, while ionic bond is determined by the charge transfer between atoms. The calculated total (partial) densities of states (DOS) of the three intermetallic compounds are shown in Fig. 4. It is found that the main bonding peaks of $MgCu_2$, $Mg_2Ca$ and $MgZn_2$ locate in the range from −10 eV to 0 eV, originating from the contribution of valance electron numbers of Mg s, Mg p, Cu s and Cu d orbits; Mg s, Mg p, Ca s and Ca p orbits; Mg s, Mg p, Zn s and Zn d orbits, respectively. From Fig. 4, it can be seen that for $MgCu_2$, orbits are mainly Mg s state and Cu s state hybrid; for $Mg_2Ca$, orbits are Mg s, p state and Cu s state hybrid; for $MgZn_2$, orbits are Mg s state and Zn s state hybrid. From the perspective of covalent bond, the stability of $Mg_2Ca$ phase is stronger than that of $MgCu_2$ or $MgZn_2$, which are not entirely consistent with cohesive energy results. Therefore, it needs to consider the ionic bond feature of the three intermetallic compounds.

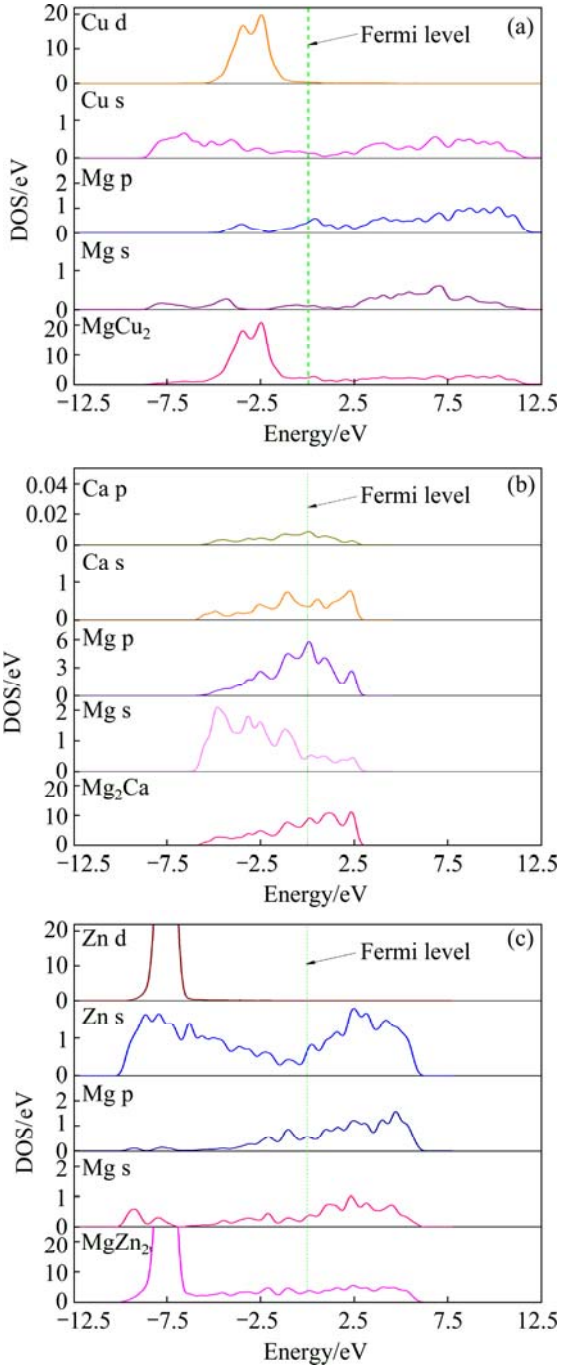


**Fig. 4** Density of states (DOS) of $MgCu_2$ (a), $Mg_2Ca$ (b) and $MgZn_2$ (c)

The Mulliken population of $MgCu_2$, $Mg_2Ca$ and $MgZn_2$ are tabulated in Table 6. Mg−Zn(1) represents the chemical bonds between Mg and the nearest neighbor Zn atom, Mg−Zn(2) represents the chemical bonds between Mg and the farthest Zn atom. If the chemical bond length is positive, the chemical bond in the compound can be built. From Table 6, we can know that the chemical bonds of these compounds are able to build, due to the fact that the bond lengths of these compounds are all positive. There are six types of chemical bonds in $Mg_2Ca$ and the populations of $Mg_2Ca$ are all positive. Hence, these data illustrate that the covalency of chemical bonds is strong in $Mg_2Ca$. In $MgZn_2$, the population of Mg−Zn(2) is −0.20. Comparing $MgZn_2$ with $Mg_2Ca$, it can be found that the covalency of chemical bonds in $MgZn_2$ is weaker than that in $Mg_2Ca$. There are three types of chemical bonds in $MgCu_2$ and the population of Mg−Mg, Mg−Cu and Cu−Cu bonds are −0.08, −0.13 and 0.53, respectively. It can be known that the metallicity of chemical bonds is significantly enhanced in $MgCu_2$.

The electron occupation numbers of $MgCu_2$, $Mg_2Ca$ and $MgZn_2$ are shown in Table 7. It is found that for $MgCu_2$, the valence electron configuration of Mg atom is $2p^63s^2$; the electron configuration of Mg is $2p^{6.35}3s^{0.4}$ obtained through calculation; the electronic number localized in Mg atom is 6.74; and the lost electron number of Mg is 0.75 e. The valence electron configuration of Cu is $3d^{10}4s^1$; after optimization, the electron configuration of Cu is $3d^{9.75}4s^{0.72}$; the electronic number localized in Cu is 11.63; the obtained electron number of Cu is 0.63 e. Similarly, for $Mg_2Ca$, the lost electron number of Ca is 0.9 e; the obtained electron number of Mg are 0.37 e and 0.48 e, respectively. For $MgZn_2$, the lost electron number of Mg is 1.03 e; the obtained electron number of Zn is 0.46 e and 0.53 e, respectively. For $MgCu_2$, the charge transfer from Mg atoms to Cu atoms and the transfer number is 5.04 (1.26×4). For $Mg_2Ca$, the charge transfers from Ca atoms to Mg atoms, and the transfer number is 3.60 (0.90×4). For $MgZn_2$, the charge transfers from Mg atoms to Zn atoms, and the transfer number is 4.12 (1.03×4). Hence, the ionic bonds of the three intermetallic compounds from strong to weak are: $MgCu_2$, $MgZn_2$ and $Mg_2Ca$.

**Table 6** Mulliken population analysis of $MgCu_2$, $Mg_2Ca$ and $MgZn_2$

| $MgCu_2$ | | | $Mg_2Ca$ | | | $MgZn_2$ | | |
|---|---|---|---|---|---|---|---|---|
| Bond | Population | Length/Å | Bond | Population | Length/Å | Bond | Population | Length/Å |
| Mg−Mg | −0.08 | 3.057 | Mg−Mg(1) | 0.58 | 3.086 | Mg−Mg(1) | 0.17 | 3.182 |
| | | | Mg−Mg(2) | 0.16 | 3.122 | Mg−Mg(2) | 0.06 | 3.215 |
| Mg−Cu | −0.13 | 2.927 | Mg−Ca(1) | 0.04 | 3.627 | Mg−Zn(1) | 0.00 | 3.048 |
| | | | Mg−Ca(2) | 0.23 | 3.660 | Mg−Zn(2) | −0.20 | 3.072 |
| Cu−Cu | 0.53 | 2.496 | Ca−Ca(1) | 0.03 | 3.815 | Zn−Zn(1) | 1.17 | 2.552 |
| | | | Ca−Ca(2) | 0.02 | 3.819 | Zn−Zn(2) | 0.06 | 2.633 |

**Table 7** Mulliken charge of $MgCu_2$, $Mg_2Ca$ and $MgZn_2$

| Phase | Species | Mulliken charge/e | | | Total change/e | Charge change/e |
|---|---|---|---|---|---|---|
| | | s | p | d | | |
| $MgCu_2$ | Mg | 0.40 | 6.35 | 0.00 | 6.74 | 1.26 |
| | Cu | 0.72 | 1.16 | 9.75 | 11.63 | –0.63 |
| $Mg_2Ca$ | Mg(I) | 0.92 | 7.45 | 0.00 | 8.37 | –0.37 |
| | Mg(II) | 0.93 | 7.55 | 0.00 | 8.48 | –0.48 |
| | Ca | 2.44 | 6.00 | 0.66 | 9.10 | 0.90 |
| $MgZn_2$ | Mg | 0.51 | 6.46 | 0.00 | 6.97 | 1.03 |
| | Zn(I) | 0.72 | 1.79 | 9.95 | 12.46 | –0.46 |
| | Zn(II) | 0.78 | 1.81 | 9.95 | 12.53 | –0.53 |

In this work, to further reveal the covalent and ionic bonding characteristics, the charge density difference is investigated. Charge density difference can directly reflect the bonding characteristics. The results are shown in Fig. 5. The contour lines are plotted from −0.2 e/Å$^3$ to 0.2 e/Å$^3$ with 0.1 e/Å$^3$ interval. From Fig. 5(a), the bonding between Cu and its adjacent Cu atom is mainly covalent, the bonding between Cu and Mg is ionic and the bonding between Mg and Mg is metallic. In Fig. 5(b), the bonding between Mg and its nearest Mg atom is covalent, the bonding between Mg and Ca is ionic and the bonding between Ca and Ca is metallic. In Fig. 5(c), it is found that there are covalent Zn−Zn bonds, ionic Mg−Zn bonds and metallic Mg−Mg bonds. Generally, for $AB_2$ type Laves intermetallic compounds, there are mainly metallic bonding between A atoms, covalent bonding between B atoms and ionic bonding between A and B atoms. Based on the above discussion, the bonding characteristics of $MgCu_2$, $Mg_2Ca$ and $MgZn_2$ are all covalent bonds, ionic bonds and metallic bonds, which lead to the structural stability.

The metallicity of $MgCu_2$, $Mg_2Ca$ and $MgZn_2$ are calculated by [34]

$$f_m = \frac{n_m}{n_e} = \frac{k_B T D_f}{n_e} = \frac{0.026 D_f}{n_e} \quad (17)$$

where $D_f$ is the DOS value at Fermi level; $T$ is the temperature; $k_B$ is the Boltzmann constant; $n_m$ and $n_e$ are the densities of the thermal excited electrons and valence electron in the cell, respectively. $n_e$ is calculated by $n_e=N/V$, where $N$ is the total number of valence electrons and $V$ is the cell volume. The relevant parameters and calculated results are listed in Table 8, from which we can obtain that metallic strength in ascending order is: $MgZn_2$< $MgCu_2$<$Mg_2Ca$.

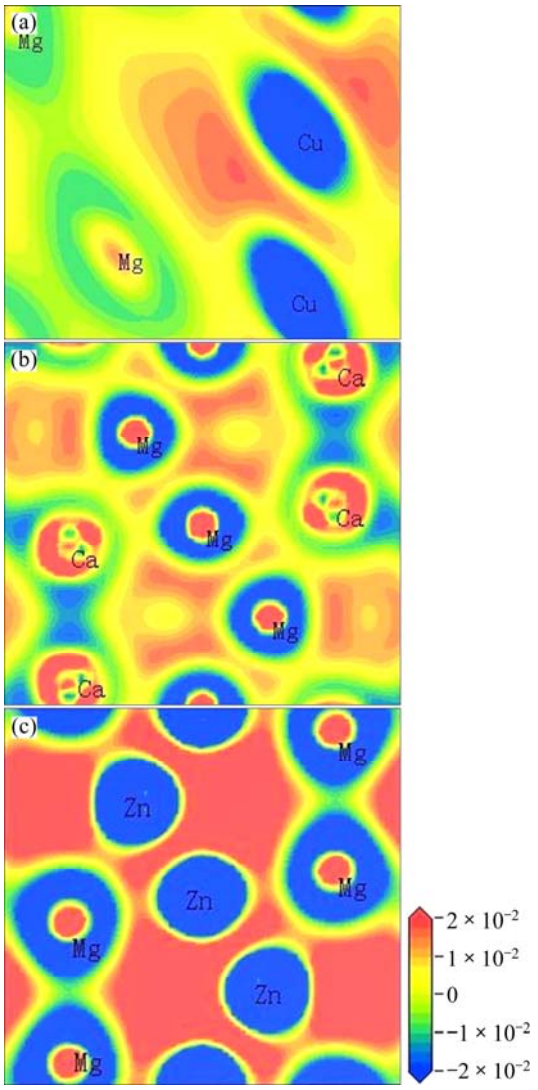


**Fig. 5** Electron density difference of $MgCu_2$ (a), $Mg_2Ca$ (b) and $MgZn_2$ (c) (The interpretation of these color maps are shown in charge density contours from −0.2 to 0.2 e/Å$^3$)

**Table 8** Density of states at Fermi level $D_f$, total number of valence electrons $N$, cell volume $V$ and metallicity parameter ($f_m$) of $MgCu_2$, $Mg_2Ca$ and $MgZn_2$

| Phase | $D_f$/(eV·atom) | $N$ | $V$/Å$^3$ | $f_m$ |
|---|---|---|---|---|
| $MgCu_2$ | 2.2804 | 48.039 | 351.789 | 0.434 |
| $Mg_2Ca$ | 8.9372 | 23.803 | 342.209 | 3.341 |
| $MgZn_2$ | 3.6901 | 104.054 | 199.922 | 0.184 |

### 3.5 Debye temperature

After the elastic constants and electronic structures of the alloys are got, Debye temperature ($\Theta_D$) can be calculated at low temperature. Debye temperature of materials gives some insight into the thermodynamics deduced from elastic constants. It is known that the Debye temperature can be used to represent the strength of covalent bond in solids. The Debye temperatures of $MgCu_2$, $Mg_2Ca$ and $MgZn_2$ are calculated using the average sound velocity ($v_m$) by the following equation [35,36]:

$$\Theta_D = \frac{h}{k_B}\left[\frac{3n}{4\pi}\left(\frac{N_A\rho}{M}\right)\right]^{1/3}\cdot v_m \quad (18)$$

where $h$ is the Planck constant; $k_B$ is the Boltzmann constant; $N_A$ is the Avogadro number; $n$ is the total number of atoms per formula; $\rho$ (=$M/V$) is the density, where $M$ is the molecular mass per formula. The average wave velocity ($v_m$) in the polycrystalline material can be calculated by

$$v_m = \left[\frac{1}{3}\left(\frac{2}{v_s^3}+\frac{1}{v_l^3}\right)\right]^{-1/3} \quad (19)$$

where $v_l$ and $v_s$ are the longitudinal and shear sound velocities, respectively, which are gained from the values of Hill's bulk moduli $B$ and shear moduli $G$ from Navier's equation [37]:

$$v_l = \sqrt{\left(B+\frac{4}{3}G\right)\frac{1}{\rho}},\quad v_s = \sqrt{G/\rho} \quad (20)$$

The calculated results of longitudinal sound velocity $v_l$, shear sound velocity $v_s$, average sound velocity $v_m$ and Debye temperature $\Theta_D$ are listed in Table 9, the calculated averaged elastic wave velocity of $MgCu_2$ or $Mg_2Ca$ is larger than that of $MgZn_2$, which is around 3000 m/s. A reasonable explanation is that these compounds have large bulk moduli ($B$) and shear moduli ($G$) values. The Debye temperature of $MgCu_2$ is estimated to be 315.57 K, which agrees well with the available value 332.5 K [38] derived by specific heat capacity measurements and 336.40 K [38], 339 K [39] obtained by elasticity measurements. The obtained result of $MgZn_2$ here is 207.62 K, which is close to the theoretical value of 259.46 K [40]. The little error is due to the smaller values of $B$ and $G$ calculated here. By now, we cannot find any other Debye temperature values of $Mg_2Ca$ comparison, but due to the credibility values of $MgCu_2$ and $MgZn_2$, we can say that the value of $Mg_2Ca$ is available. The largest $\Theta_D$ is 328.70 K for $Mg_2Ca$. The larger the Debye temperature is, the stronger the covalent bond strength in solids is [41]. From Table 8, we can summarize that the covalent bond in $Mg_2Ca$ is the strongest among these phases, which is consistent with the results of density of states (DOS) in section 3.4 that $Mg_2Ca$ has the strongest covalent bond.

**Table 9** Theoretically calculated thermal properties of $MgCu_2$, $Mg_2Ca$ and $MgZn_2$ phases, including density ($\rho$), longitudinal sound velocity ($v_l$), shear velocity ($v_s$), average sound velocity ($v_m$) and Debye temperature ($\Theta_D$)

| Phase | $\rho$/(g·cm$^{-3}$) | $v_l$/(m·s$^{-1}$) | $v_s$/(m·s$^{-1}$) | $v_m$/(m·s$^{-1}$) | $\Theta_D$/K |
|---|---|---|---|---|---|
| $MgCu_2$ | 5.72 | 4803.97 | 2310.28 | 2597.33 | 315.57 |
| $Mg_2Ca$ | 1.72 | 5412.63 | 3023.17 | 3365.63 | 328.70 |
| $MgZn_2$ | 5.15 | 4078.28 | 1567.26 | 1777.41 | 207.62 |

## 4 Conclusions

1) The calculated lattice parameters are good consistent with the experimental and literature values. The calculated heat of formation and cohesive energies show that $MgCu_2$ has stronger alloying ability and structural stability than $Mg_2Ca$ and $MgZn_2$.

2) The elastic constants of $MgCu_2$, $Mg_2Ca$ and $MgZn_2$ phases are calculated. The results of bulk moduli $B$, shear moduli $G$, elastic moduli $E$ and Poisson ratio $v$ show that $MgCu_2$ has stronger deformation resistant capacity than $Mg_2Ca$ and $MgZn_2$, the plasticity of $MgZn_2$ phase is the best, the stiffness of $MgCu_2$ is the largest and $MgCu_2$, $Mg_2Ca$ and $MgZn_2$ are all ductile phases.

3) The melting points of $MgCu_2$,$Mg_2Ca$ and $MgZn_2$ phases are predicted using the cohesive energy and elastic constants based on the empirical formula. The calculated results show that $MgCu_2$ has the highest melting point.

4) The bonding characteristics of $MgCu_2$, $Mg_2Ca$ and $MgZn_2$ are all covalent, ionic and metallic, respectively.

5) The Debye temperatures obtained by the elastic constants are calculated and the results show that $Mg_2Ca$ has the strongest covalent bond.

## References

[1] HE S M, ZENG X Q, PENG L M, GAO X, NIE J F, DING W J. Microstructure and strengthening mechanism of high strength

Mg−10Gd−2Y−0.5Zr alloy [J]. J Alloy Compd, 2007, 427: 316−323.

[2] SMOLA B, STULIKOVA I, von BUCH F, MORDIKE B L. Structural aspects of high performance Mg alloys design [J]. Mater Sci Eng A, 2002, 324: 113−117.

[3] ZHOU Tao, CHEN Zhen-hua, YANG Ming-bao, HU Jian-jun, XIA Hua. Investigation on microstructure characterization and property of rapidly solidified Mg−Zn−Ca−Ce−La alloys [J]. Mater Characterization, 2012, 63: 77−82.

[4] ЛЯКИШЕВ Н П. Metal binary system manual [M]. GUO Qing-wei. Beijing: Chemical Industry Press, 2009. (in Chinese)

[5] ZENG Xiao-qin, ZHANG Ya, LU Chen, DING Wen-jiang, WANG Ying-xin, ZHU Yan-pin. Precipitation behavior and mechanical properties of a Mg−Zn−Y−Zr alloy processed by thermo-mechanical treatment [J]. J Alloys Compd, 2005, 395: 213−219.

[6] NIMITYONGSKUL S, JONES M, CHOI H, LAKES R, KOU S, LI X C. Grain refining mechanisms in Mg−Al alloys with $Al_4C_3$ microparticles [J]. Mater Sci Eng A, 2010, 527: 2104−2111.

[7] OH-ISHI K, MENDIS C L, HOMMA T, KAMADO S, OHKUBO T, HONO K. Bimodally grained microstructure development during hot extrusion of Mg−2.4Zn−0.1Ag−0.1Ca−0.16Zr (at.%) alloys [J]. Acta Mater, 2009, 57: 5593−5604.

[8] ZHANG Bao-ping, WANG Yin, GENG Lin, LU Chun-xiang. Effects of calcium on texture and mechanical properties of hot-extruded Mg−Zn−Ca alloys [J]. Mater Sci Eng A, 2012, 539: 56−60.

[9] TONG L B, ZHENG M Y, HU X S, WU K, XU S W, KAMADO S, KOJIMA Y. Influence of ECAP routes on microstructure and mechanical properties of Mg−Zn−Ca alloy [J]. Mater Sci Eng A, 2010, 527: 4250−4256.

[10] LUO A, PEKGULERYUZ M O. Cast magnesium alloys for elevated temperature applications [J]. J Mater Sci, 1994, 29: 5259−5271.

[11] QIU Ke-qiang, WANG Meng, ZHANG Hong-bing, BAI Xiao-jun, REN Ying-lei, ZHANG Tao. Effect of Cu on glass forming ability and mechanical properties of Mg−Zn−Ca alloys [J]. The Chinese Journal of Nonferrous Metals, 2009, 19(4): 677−680. (in Chinese)

[12] SENKOV O N, SCOTT J M. Formation and thermal stability of Ca−Mg−Zn and Ca−Mg−Zn−Cu bulk metallic glasses [J]. Mater Lett, 2004, 58: 1375−1378.

[13] LIU Yong, HU Wen-cheng, LI De-jiang, ZENG Xiao-qin, XU Chun-shui, YANG Xiang-jie. First-principles investigation of structural and electronic properties of $MgCu_2$ Laves phase under pressure [J]. Intermetallics, 2012, 31: 257−263.

[14] FAST L, WILLS J M, JOHANSSON B, ERIKSSON O. Elastic constants of hexagonal transition metals: Theory [J]. Phys Rev B, 1995, 51: 17431−17438.

[15] SHI D M, WEN B, MELNIK R, YAO S, LI T J. First-principles studies of Al−Ni intermetallic compounds [J]. J Solid State Chem, 2009, 182: 2664−2669.

[16] PERDEW J P, BURKE K, ERNZERHOF M. Generalized gradient approximation made simple [J]. Phys Rev Lett, 1996, 77: 3865−3868.

[17] FAGAN S B, MOTA R, BAIERLE R J, PAIVA G, da SILVA J R, FAZZIO A. Stability investigation and thermal behavior of a hypothetical silicon nanotube [J]. J Mol Struct, 2001, 539: 101−106.

[18] GANESHAN S, SHANG S L, ZHANG H, WANG Y, MANTINA M, LIU Z K. Elastic constants of binary Mg compounds from first-principles calculations [J]. Intermetallics, 2009, 17: 313−318.

[19] ZHOU Dian-wu, XU Shao-hua, ZHANG Fu-quan, PENG Ping, LIU Jin-shui. First-principles calculations of structural stabilities and elastic properties of $AB_2$ type intermetallics in ZA62 magnesium alloy [J]. Acta Metall Sinca, 2010, 46(1): 97−103. (in Chinese)

[20] SUZUKI A, SADDOCK N D, JOMES J W, POLLOCK T M. Solidification paths and eutectic intermetallic phases in Mg−Al−Ca ternary alloys [J]. Acta Mater, 2005, 53: 2823−2834.

[21] YU Wei-yang. Electronic structure and mechanical properties of Mg−Al−Ca Laves phase and Mg−Al−Sb alloys [D]. Xiangtan: Xiangtan University, 2009. (in Chinese)

[22] HUANG Kun. Solid state physics [M]. Beijing: Higher Education Press, 1985. (in Chinese)

[23] LI C H, HOE J L, WU P. Empirical correlation between melting temperature and cohesive energy of binary Laves phases [J]. J Phys Chem Solids, 2003, 64: 201−212.

[24] ANSARA I, DINADALE A T, RAND M H. Thermodynamic database for light metal alloys [M]. Brussels: European Commission, 1998.

[25] SAHU B R. Electronic structure and bonding of ultralight LiMg [J]. Mater Sci Eng B, 1997, 49: 74−78.

[26] ZHOU Dian-wu, LIU Jin-shui, PENG Ping. A first-principles study on electronic structure and elastic properties of $Al_4Sr$, $Mg_2Sr$ and $Mg_{23}Sr_6$ phases [J]. Transactions of Nonferrous Metals Society of China, 2011, 21: 2677−2683.

[27] SUDHA PRIYANGA G, ASVINI MEENAATCI A T, RAJESWARA PALANICHAMY R, IYAKUTTI K. First principles study of structural, electronic and mechanical properties of transition metal hydrides (TMH, TM=Mo, Tc, Ru) [J]. Transactions of Nonferrous Metals Society of China, 2013, 23: 2700−2707.

[28] CORKILL J L, COHEN M L. Structural, bonding and electronic properties of IIA–IV antifluorite compounds [J]. Phys Rev B, 1993, 48: 17138−17144.

[29] SEIDENKRANZ T, HEGENBARTH E. Single-crystal elastic constants of $MgZn_2$ in the temperature range from 4.2 to 300 K [J]. Phys Status Solidi A, 1976, 33: 205−210.

[30] HILL R. The elastic behaviour of a crystalline aggregate [J]. Phys Soc Sect A, 1952, 65: 349−354.

[31] PUGH S F. Relations between the elastic moduli and the plastic properties of polycrystalline pure metals [J]. Philos Mag, 1954, 45: 823−843.

[32] FU C L, WANG X D, YE Y Y, HO K M. Phase stability, bonding mechanism, and elastic constants of $Mo_5Si_3$ by first-principles calculation [J]. Intermetallics, 1999, 7: 179−184.

[33] PAN Liu-xian, XIA Qing-lin, YE Shao-long, DING Ning, LIU Zi-ran. First principles study of electronic structure, chemical bonding and elastic properties of BiOCuS [J]. Transactions of Nonferrous Metals Society of China, 2012, 22: 1197−1202.

[34] HUANG Z W, ZHAO Y H, HOU H, HAN P D. Electronic structural, elastic properties and thermodynamics of $Mg_{17}Al_{12}$, $Mg_2Si$ and $Al_2Y$ phases from first-principles calculations [J]. Physica B, 2012, 407: 1075−1081.

[35] SIN'KO G V, SMIRNOV N A. Ab initio calculations of elastic constants and thermodynamic properties of BCC, FCC, and HCP Al crystals under pressure [J]. J Phys: Condense Matter, 2002, 14: 6989−7005.

[36] ANDERSON O L. A simplified method for calculating the Debye temperature from elastic constants [J]. J Phys Chem Solids, 1963, 24: 909−917.

[37] WACHTER P, FILZMOSER M, REBIZANT J. Electronic and elastic properties of the light actinide tellurides [J]. Physica B, 2001, 293: 199−223.

[38] SHANNETTE G W, SMITH J F. Single crystalline elastic constants of cubic $MgCu_2$, $MgZn_2$ alloys [J]. J Appl Phys, 1971, 42: 2793−2799.

[39] SIETHOFF H, AHLBORN K. Debye-temperature−elastic-constants relationship for materials with hexagonal and tetragonal symmetry

[J]. J Appl Phys, 1996, 79: 2968−2974.

[40] CHEN Qiang, HUANG Zhi-wei, ZHAO Zu-de, SHU Da-yu. First principles study on elastic properties, thermodynamics and electronic structural of $AB_2$ type phases in magnesium alloy [J]. Solid State Commun, 2013, 162: 1−7.

[41] LI Ye-fei, GAO Yi-min, XIAO Bing, MIN Ting, FAN Zi-jian, MA Sheng-qiang, XU Lei-lei. Theoretical study on the stability, elasticity, hardness and electronic structures of W−C binary compounds [J]. J Alloys Compd, 2010, 502: 28−37.

# $MgCu_2$, $Mg_2Ca$ 和 $MgZn_2$ Laves 相力学性质和电子结构的第一性原理计算

毛萍莉，于 波，刘 正，王 峰，鞠 阳

沈阳工业大学 材料科学与工程学院，沈阳 110870

**摘 要**：通过基于密度泛函理论的第一性原理计算方法，对 $MgCu_2$, $Mg_2Ca$ 和 $MgZn_2$ 的力学性能和电子结构进行计算，计算所得晶格参数与实验值和文献值相吻合。合金形成热和结合能的计算结果表明，$MgCu_2$ 具有最强的合金形成能力和结构稳定性。计算了 $MgCu_2$, $Mg_2Ca$ 和 $MgZn_2$ 的弹性常数，推导了体模量、剪切模量、弹性模量和泊松比。结果表明，$MgCu_2$、$Mg_2Ca$ 和 $MgZn_2$ 均为延性相，$MgCu_2$ 的刚度最大，$MgZn_2$ 的塑性最好。通过对结合能和弹性常数的计算，预测了 $MgCu_2$、$Mg_2Ca$ 和 $MgZn_2$ 的熔点。通过对态密度(DOS)、Mulliken 布居数、电子占据数和差分电荷密度的计算，分析了 $MgCu_2$、$Mg_2Ca$ 和 $MgZn_2$ 的结构稳定性和力学性能机制。最后，计算和讨论了 3 种金属间化合物的 Debye 温度。

**关键词**：镁合金；$MgCu_2$；$Mg_2Ca$；$MgZn_2$；Laves 相；电子结构；力学性能；Debye 温度

**(Edited by Hua YANG)**